



ELSEVIER

Available online at www.sciencedirect.com

Journal of Volcanology and Geothermal Research xx (2007) xxx–xxx

Journal of volcanology
and geothermal researchwww.elsevier.com/locate/jvolgeores

Volcanic emissions from Popocatepetl volcano, Mexico, quantified using Moderate Resolution Imaging Spectroradiometer (MODIS) infrared data: A case study of the December 2000–January 2001 emissions

M.A. Matiella Novak ^{a,*}, I.M. Watson ^{a,b}, H. Delgado-Granados ^c, W.I. Rose ^a,
L. Cárdenas-González ^d, V.J. Realmuto ^e

^a Department of Geological and Mining Engineering and Sciences, Michigan Technological University, 1400 Townsend Drive, Houghton, MI, 49931-1295, USA

^b Department of Earth Sciences, University of Bristol, Queen's Rd, Bristol, BS8 1RJ, UK

^c Instituto de Geofísica, UNAM, Circuito Científico C. U. Coyoacán 04510, México, D. F.

^d Centro Nacional de Prevención de Desastres, Delfín Madrigal 665, Coyoacán 04360 México, D.F.

^e Jet Propulsion Laboratory, 4800 Oak Grove Dr. Pasadena, CA 91109, USA

Received 6 September 2007

Abstract

During December 2000 and January 2001, an increase in activity at Popocatepetl volcano, Mexico, was observed in both ground-based correlation spectrometer (COSPEC) data and in imagery from various satellite sensors, including the Moderate Resolution Imaging Spectroradiometer (MODIS), Total Ozone Mapping Spectrometer (TOMS), Advanced Very High Resolution Radiometer (AVHRR), and Geostationary Satellite 8 (GOES-8). Fine ash abundances detected by MODIS ranged between 6000 and 255,000 metric tons, and fine ash abundances detected by AVHRR, measured at different times, ranged between 4000 and 76,000 metric tons. The difference in ranges of ash mass detected by these two sensors depends largely on the difference in data acquisition time between the two sensors in detecting Popocatepetl's ash clouds. However, the difference could also be partly attributed to differences in spatial resolution and band sensitivity, which are believed to be significantly more favorable for MODIS. Mean effective radii for the two sensors images were typically within 10% of each other; values ranged from 5 to 8 μm and were strongly a function of residence time.

Two types of infrared retrieval were used for the detection and quantification of SO_2 masses — one based on the 7.3 μm SO_2 absorption feature and the other on the 8.6 μm absorption feature. SO_2 values were attainable using the 8.6 μm retrieval for most images, but were problematic using the 7.3 μm retrieval. Only one SO_2 cloud was successfully measured by the 7.3 μm retrieval (January 23rd 2001 04:50 UTC). This cloud was at an altitude of approximately 12 km, the highest cloud in the suite of images analyzed, and yielded an SO_2 mass of 16,500 metric tons. This suggests that elevated heights — above ~ 10 km — are required to negate the effects of atmospheric water vapor upon the 7.3 μm retrieval at tropical latitudes. SO_2 clouds for which the 8.6 μm retrieval was successful but 7.3 μm was not were at heights between 6 and 10 km.

Comparison of SO_2 retrievals obtained from MODIS images directly to COSPEC measurements was achieved by taking cross sections of the plume in the MODIS SO_2 maps. Wind data at the appropriate altitude can then be used to calculate fluxes comparable to those measured by COSPEC in units of tons day^{-1} . The fluxes calculated from the plume transects fell within the range of fluxes measured by the COSPEC, at 5–32 kT day^{-1} , and suggest more emissions in mid to late December, and lower emission rates throughout January. The MODIS data also complement a ground-based study on magnetic anomalies in which it was observed that more magma was extruded in the January 23, 2001 eruption than in the eruptions in December of 2000. Ash quantification from MODIS imagery suggests that the majority of fine ash was erupted in January of 2001.

© 2007 Elsevier B.V. All rights reserved.

Keywords: Volcanic ash; SO_2 ; MODIS; infrared; Popocatepetl; remote sensing

* Corresponding author. Tel.: +906 487 2826; fax: +906 487 3371.

E-mail address: mamatiel@mtu.edu (M.A. Matiella Novak).

1. Introduction

Popocatepetl volcano is located approximately 60 km southeast of the capitol city of Mexico, Mexico City, and 45 km southwest of Puebla City (Fig. 1). These two cities in central Mexico have a combined population of more than 20 million, and Mexico City particularly is the location of significant infrastructure such as the international airport, the largest and most important in the country. With such a large population and a major airport nearby, observation of volcanic clouds from Popocatepetl on a large scale is crucial. The volcano has been passively degassing for a long period and analyzing its emissions, through ground-based measurement, is an important part of Popocatepetl's monitoring (Delgado-Granados et al., 2001).

The current eruption of Popocatepetl volcano began on December 21st, 1994, and is of Vulcanian type, with ash emissions and an anomalously large amount of passively degassed sulfur dioxide (SO₂). Previous ground-based gas-emission measurements have shown that Popocatepetl injects up to 100 kilotons (kT) a day of SO₂ (an important component of volcanic emissions) into the atmosphere and is hence one of the world's largest point sources (Goff et al., 1998; Love et al., 1998; Delgado-Granados et al., 2001). These emissions

themselves represent a significant health hazard to the large population in the close proximity to the volcano and are an important indicator of eruptive activity (Alvarez et al., 2000; Delgado-Granados et al., 2001).

Gas-emission monitoring at Popocatepetl in the last decade has mostly consisted of ground-based measurements, including measurements and volatile gas-trap studies (Goff et al., 1998), correlation spectrometer (COSPEC), and more recently, measurements using DOAS systems. Delgado-Granados et al. (2001) have stated that the SO₂ masses measured, typically at least one order of magnitude higher than observed at other large emitters of SO₂ (Andres and Kasgnoc, 1998), have “challenged the established methodologies” of measuring SO₂ emissions using the COSPEC. Moderate Resolution Imaging Spectroradiometer (MODIS) satellite imagery provides us with a large-scale perspective of volcanic emissions and atmospheric interactions, characteristics that are useful for observing larger volcanic eruptions similar to those of Popocatepetl. MODIS data provide information about Popocatepetl's volcanic clouds that are not discernible from ground-based techniques, because they can only partially observe the clouds, due to the typical scale of the emissions. The magnitude of emissions by Popocatepetl during late 2000 and early 2001 makes this



Fig. 1. Location map of Popocatepetl volcano.

eruptive sequence ideal for a case study on the detection of volcanic clouds using MODIS data.

2. MODIS imagery

The MODIS sensor used in this study is onboard NASA's Terra satellite, which was launched on December 19th, 1999. It has 36 spectral bands within the visible and infrared region of the electromagnetic spectrum (0.4–14.4 μm). It is in a polar orbiting path 705 km above the surface of the earth with a swath of 2,330 km and provides global coverage once every two days. The region of the spectrum that is used for observing volcanic clouds corresponds to bands 27 through 29, 31 and 32 of the MODIS sensor. These five bands are within the thermal infrared (TIR) between 6.535 and 12.270 μm and are sensitive to several volcanogenic species (Watson et al., 2004). Band 30 is not used in this work due to an overlying O_3 absorption feature (Realumuto et al., 1994).

MODIS images were downloaded from the NASA website, located at <http://redhook.gsfc.nasa.gov/~imswwww/pub/imswelcome/>. This website allows a registered user to select the type of satellite data they want, the location of the desired image based on latitude and longitude, and the time of the desired image. MODIS captured 33 images of Popocatepetl volcano between December 14, 2000 and January 26, 2001 during an active period at Popocatepetl when COSPEC measurements were also made. Of these images, eight were selected because the detected volcanic clouds were at least 6 km in height with little or no masking from meteorological clouds. Heights of the clouds were obtained from Washington Volcanic Ash Advisory Center (VAAC) advisories – used to re-route commercial aircraft during an eruption – and corroborated using trajectory analysis and atmospheric radiosonde data. Ash and/or SO_2 emissions during the December 2000–January 2001 eruptions were also detectable using other satellite sensors, including TOMS and AVHRR. SO_2 emission-rate measurements were also quantified with COSPEC data. Table 1 shows these various sensors and the time they observed a volcanic emission; these data are also plotted in Fig. 2a and b.

3. Infrared retrieval schemes

As previously stated, both silicate ash and SO_2 contain extinction features within the thermal infrared region of the spectrum (between 7 and 12 μm). MODIS can be used to detect the thermal infrared transmission signatures of ash, SO_2 , sulfates, and ice (Watson et al., 2004). Several algorithms have been developed to calculate the amount of SO_2 and ash within a cloud using radiative transfer models. Three of these algorithms were used for this research, utilizing the SO_2 absorption features at 7.3 μm and 8.6 μm and the difference in attenuation by ash between 11 μm and 12 μm .

The radiance model used for detecting the amount of absorption by SO_2 at 7.3 μm is henceforth referred to as the 7.3 μm retrieval (Prata et al., 2003). The radiance model used for detecting the amount of absorption by SO_2 at 8.6 μm is henceforth referred to as the 8.6 μm retrieval (Realumuto et al.,

1994, 1997, Realumuto 2000). The ash retrieval applies a technique commonly known as the “split-window” technique, which uses the brightness temperature difference of the volcanic cloud at 11 μm and 12 μm to determine the amount of ash (Prata, 1989a,b; Wen and Rose, 1994). Table 2 lists the MODIS channels that correspond to these wavelengths and references where more information about these techniques can be found. As the three algorithms are summarized and detailed extensively elsewhere (Watson et al., 2004), they will be only briefly described here.

3.1. The split-window ash retrieval for MODIS and AVHRR images

The brightness temperature difference between MODIS channels 31 and 32 (channels 4 and 5 for AVHRR images) can be related to the optical depth and effective radius (and hence the mass) using the underpinning equations:

$$L_s = e^{\tau_c} B(T_s) + (1 - e^{\tau_c}) B(T_c) \quad (1)$$

$$L_s = (1 - r_c(r_c, \tau_c)) (B(T_c) + t_c(r_c, \tau_c) (B(T_s) - B(T_c))) \quad (2)$$

where L_s is the at-sensor radiance measured, B is the Planck function, τ_c is the optical depth of the cloud, T_s is the underlying surface temperature, T_c is the cloud temperature, t_c is the transmissivity of the cloud, r_c is the reflectivity of the cloud, and r_e is the effective radius (Wen and Rose, 1994; Watson et al., 2004).

Using a pair of radiances (typically centered upon 11 and 12 μm) a look-up-table (LUT) is derived, based on the ash's refractive index, underlying surface temperature, cloud height and transmissivity. Each pixel in the image is then run through the model and an effective radius (r_e) and optical depth (τ) assigned from the LUT based on the 11 μm brightness temperature and the 11–12 μm brightness temperature difference. Once the optical depth and effective radius are calculated, it is simple to derive the mass of fine ash in each pixel using the density of the material (Wen and Rose, 1994).

3.2. The 8.6 μm SO_2 retrieval

The success of this technique depends on being able to accurately characterize (i) the surface beneath the plume, (ii) the atmosphere in the path and (iii) the plume geometry (height and thickness). The 8.6 μm retrieval first necessitates designation of an SO_2 -free background region. Then, the spectral emissivity and ground temperature of the ground beneath an SO_2 -free, user-defined atmosphere can be calculated. The ‘apparent’ ground temperature is then calculated for an SO_2 -laden atmosphere assuming an identical background emissivity. The difference in apparent ground temperature between an SO_2 -free region and one containing SO_2 directly relates to the amount of SO_2 in the cloud studied, if the atmosphere and the cloud height are defined according to

$$L_s = \{ \varepsilon_g B(T_s) + (1 - \varepsilon_g) L_d \} t_a + L_u \quad (3)$$

Table 1
Dates and times of satellite-sensor observations of the clouds

Sensor	MODIS		AVHRR		TOMS		GOES-8	
Spatial resolution	1 km		1.1 km		39 km		4 km	
Dates and times (UTM)	12/14/00	17:50	12/14/00	22:59	12/15/00	00:28	12/14/00	19:15
	12/15/00	16:55	12/15/00	22:47	12/19/00	00:43	12/15/00	20:02
	12/16/00	05:30	12/17/00	23:06	12/20/00	01:37	12/16/00	08:15
	12/19/00	04:20	12/19/00	22:02	12/21/00	00:31	12/19/00	02:15
	12/20/00	05:05	01/22/01	23:43	12/22/00	00:05	12/20/00	07:02
	12/20/00	17:15					12/20/00	18:45
	01/23/01	04:50					01/23/01	05:15
	01/23/01	17:00					01/23/01	16:02

where ϵ_g is the emissivity of the ground, T_s is the surface temperature, L_d is the ground welling radiance, t_a is the transmissivity of the atmosphere and L_u is the upwelling radiance. The retrieval is confounded by the presence of radiatively active species, such as ash and aerosols and by errors in poorly constrained plume geometry and atmospheric conditions. Any disparity between the ‘true’ and ‘apparent’ ground temperature is mapped as SO_2 , leading to a likely overestimate in the SO_2 burden. A map of the SO_2 column abundance is derived for an area within the MODIS scene, which can again be straightforwardly converted into a total SO_2 cloud mass.

3.3. The 7.3 μm SO_2 retrieval

The 7.3 μm retrieval works similarly to the 8.6 μm retrieval as it uses an absorption signature of SO_2 and reference channels (in this case channels 27 and 31). However, channels 27 and 28 are vertical sounding channels (i.e., they are masked by a H_2O absorption feature and do not observe the ground) and thus only detect emission from the atmosphere (specifically water vapor) at a height of about 3–5 km. This means that all absorption from SO_2 below this altitude cannot be quantified. Emission by water vapor at the sounding altitude is used as the source to detect absorption by SO_2 above that level. The height of the SO_2 cloud must be input so that the program can assign a temperature to the cloud top. A synthetic channel at 7.3 μm is derived from linear interpolation of the radiance values of channels 27 and 31. The difference between this radiance and that of the image is a

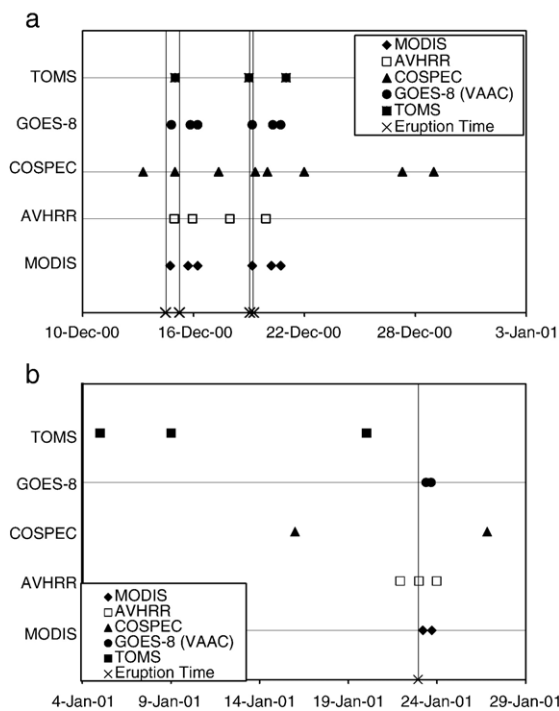


Fig. 2. Timeline of the various data collected for Popocatepetl volcano for a) December 2000 and b) January 2001. The December eruptive events mark the time of maximum intensity; however, the December 2000 eruptive phase was almost continuous for several days.

Table 2
Brief description and references of the three algorithms used in this study for SO_2 and ash detected by MODIS images

MODIS channel	Wavelength (μm)	Target species	Brief description	References
28	7.2–7.5	SO_2	Amount of SO_2 is related to the difference in radiance of SO_2 filled atmosphere and radiance of SO_2 free atmosphere.	Prata et al. (2003)
29	8.4–8.7	SO_2	Amount of SO_2 is related to the difference in radiance of clear ground and radiance of ground with SO_2 cloud over it.	Realmuto et al. (1994) Realmuto et al. (1997) Realmuto (2000) Realmuto and Worden (2000)
31, 32	10.8–11.3, 11.8–12.3	Ash	Amount of ash is related to a negative brightness temperature difference from 11 to 12 μm .	Prata (1989a,b) Wen and Rose (1994) Yu et al. (2002)

Table 3
Volcanic ash retrieval (VAR) results for MODIS and AVHRR images at Popocatepetl

Sensor	MODIS	VAR results (metric tons)	AVHRR	VAR results (metric tons)
Dates and times	12/14/00 17:50	43,000	12/14/00 22:59	14,000
	12/15/00 16:55	29,000	12/15/00 22:47	6,000
	12/16/00 05:30	40,000	12/17/00 23:06	4,000
	12/19/00 04:20	68,000	12/19/00 22:02	34,000
	12/20/00 05:05	256,000		
	12/20/00 17:15	151,000		
	01/23/01 04:50	72,000	01/22/01 23:43	76,000
	01/23/01 17:00	6,000		

Table 4
Volcanic ash retrieval (VAR) and mean effective radius (MER) results for MODIS and AVHRR images

Sensor	MODIS	VAR–MER (μm)	AVHRR	VAR–MER (μm)
Date and time	12/14/00 17:50	7.2	12/14/00 22:59	6.9
	12/15/00 16:55	5.6	12/15/00 22:47	5.7
	12/16/00 05:30	7.0	12/17/00 23:06	5.3
	12/19/00 04:20	8.0	12/19/00 22:02	6.0
	12/20/00 05:05	7.6		
	12/20/00 17:15	7.5		
	01/23/01 04:50	6.0	01/22/01 23:43	8.0
	01/23/01 17:00	6.7		

function of the SO₂ burden in the cloud as given (after Prata et al., 2003) by

$$L_{s(7.3)} - L_a = (1 - t_s)(B(T_c) - L_a) \quad (4)$$

Where $L_{s(7.3)}$ is the at-satellite radiance at 7.3 μm, t_s is the transmissivity of the SO₂ cloud, $B(T_c)$ is the Planck radiance of the SO₂ cloud and L_a is the radiance of the synthetic channel.

4. Results

4.1. Comparison between AVHRR and MODIS ash retrievals

An overview of the ash retrieval results from the MODIS and AVHRR images can be found in Table 3 and seen in Fig. 3. The volcanic ash retrieval program used for this study is referred to as VAR in the tables. The ash retrieval algorithm works similarly for both sensors, subtracting the brightness temperature corresponding to 12 μm from the brightness temperature corresponding to 11 μm and deriving the mass from this temperature difference and the 11 μm brightness temperature (Wen and Rose, 1994), so the resulting values should in theory be similar to each other, although a difference in values may arise from the differing spatial resolution (Table 1), spectral sensitivity (a NEΔT of 0.05 K for MODIS as opposed to 0.12 K for AVHRR) and/or coverage.

Examining this table and graph, the first noticeable difference among retrievals from the two sensors is that most of the plumes imaged by AVHRR detected significantly less ash than those imaged by MODIS. Upon further inspection, the data show that those AVHRR images were typically acquired within a few hours after the MODIS images (Fig. 2). These abundance differences could be because the larger ash particles fall out quickly, which means that AVHRR should detect a cloud with a smaller mean effective radius than those in the MODIS images, and this does appear to be the case (Table 4). Furthermore, the January 22, 2001 AVHRR image was taken before the January 23, 2001 MODIS image and shows a slightly higher abundance of ash and has a larger effective radius (Tables 3 and 4) corroborating this theory.

4.2. Comparison of the 7.3 and 8.6 μm SO₂ retrieval

Both 7.3 μm and 8.6 μm SO₂ retrievals were performed on the eight MODIS images. The 8.6 μm retrieval was able to detect SO₂ clouds more often than the 7.3 μm retrieval. Only in the January 23, 2001 image at 0450 UTC was absorption at 7.3 μm by SO₂ observed (Fig. 4). SO₂ in this channel was detected in a 12 km-high cloud, and the lower SO₂ clouds (at 7 km) within the image were not detected by the 7.3 μm retrieval. The SO₂ mass detected by the 7.3 μm retrieval was about 16,500 T, which is significantly less than the 53,100 T of SO₂ detected using the 8.6 μm algorithm (Table 5). This cloud

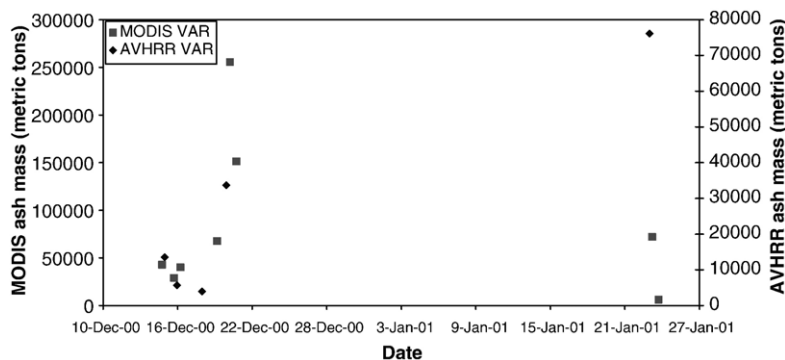


Fig. 3. Volcanic ash retrieval measurements for MODIS and AVHRR. Although actual ash values are different, increases and decreases of ash detection by the two sensors are similar.

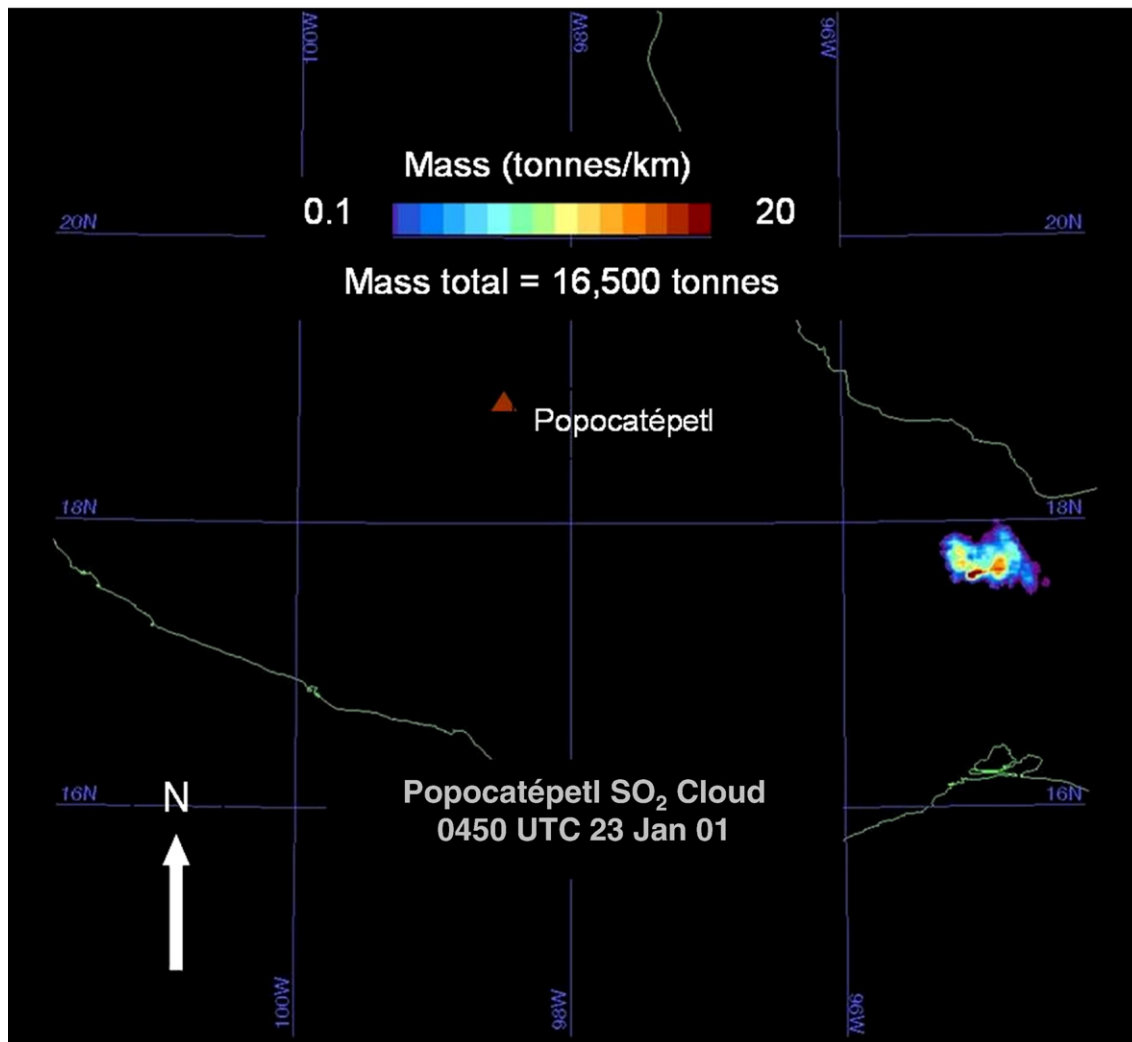


Fig. 4. SO₂ map from the 7.3 μm retrieval of the January 23rd 2001 0450 UTC image showing the cloud at 12 km height.

was the highest cloud detected in all the images and was also the highest portion of the cloud(s) observed in the 22nd January image. This suggests that the lower value derived from the 7.3 μm algorithm was due to partial detection of the cloud. Indeed, if only the highest portion of the cloud is considered, then the algorithms are in very good agreement — 16.5 kT ± 3 kT.

Clouds in other images at altitudes of 7–10 km were not detected by the 7.3 retrieval possibly because of interference from atmospheric water vapor, which was thought not to be a concern at heights above 5 km, because the majority of atmospheric water vapor is contained in the bottom 5 km of the atmosphere (Prata et al., 2003). It may also be that the height assignments, based on cloud top temperatures and trajectory analysis, were too high. This would have the effect of making the SO₂ (a) harder to detect and (b) warmer than the retrieval suggests, both effects reducing the amount of SO₂ retrieved.

The 8.6 μm retrieval was more able to detect SO₂, regardless of cloud height, because the 8.6 μm channel can detect ground-leaving radiance and has no atmospheric penetration limit. An SO₂ cloud was not detectable in only one image, the December 19, 2000 image at 04:20 UTC. The ash retrieval for this image

did reveal a large ash cloud, but SO₂ may have already converted to aerosol by the time the MODIS image was taken or the ash somehow confounded the SO₂ retrieval. As the image was acquired just after a large eruption it seems unlikely that little or no SO₂ was erupted. Large fluxes of SO₂ were detected by COSPEC (117 kT day⁻¹) and suggest, by inference that it was an explosive eruption, probable interference of ash in the SO₂ retrieval.

Table 5
SO₂ 8.6 μm retrieval for MODIS images

MODIS date and time		8.6 μm retrieval results (T)
12/14/00	17:50	11,600
12/15/00	16:55	8,700
12/16/00	05:30	Too small to estimate
12/19/00	04:20	No SO ₂ cloud detected
12/20/00	05:05	16,000
12/20/00	17:15	10,200
01/23/01	04:50	53,100
01/23/01	17:00	2,000

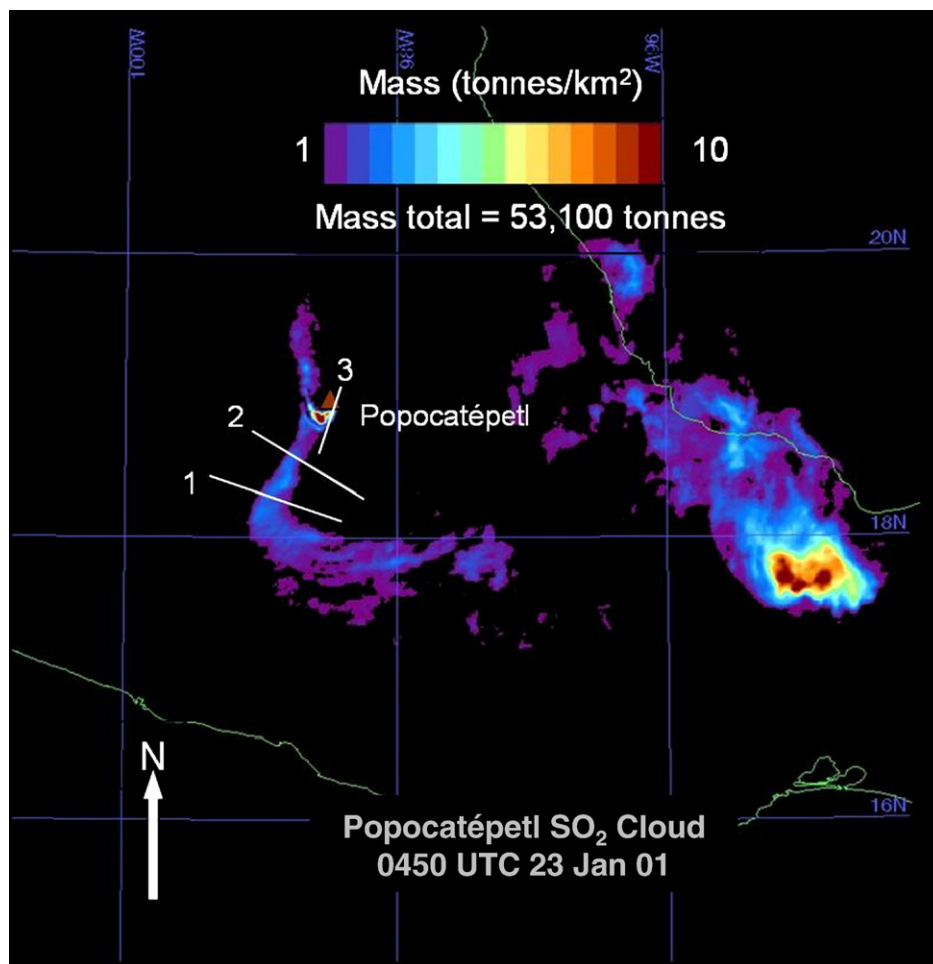


Fig. 5. Transects taken at three locations of the SO₂ cloud for the January 23rd 2001 0450 UTC image for COSPEC comparison.

4.3. MODIS transects and COSPEC comparison

COSPEC measurements were taken throughout the eruptive period and peaked on December 17, 2000, with fluxes of about 170,000 T per day (Delgado-Granados et al., 2001). This measured flux is almost two orders of magnitudes greater than the average daily output of SO₂ for Popocatépetl volcano (Delgado-Granados et al., 2001). COSPEC measurements made approximately 4 h after the December 19, 2001 MODIS image was taken (08:08 UTC) resulted in a flux of approximately 117,000 T per day. TOMS data are also available for this day, taken at 17:24 UT, and show an SO₂ cloud with a mass of about 26,000 T. Table 5 shows the SO₂ values calculated by the 8.6 μm retrieval for the MODIS images (except the December 19, 2001 image mentioned above). Values derived from satellite imagery are difficult to correlate directly with COSPEC measurements because of the difference in measurement units (8.6 μm retrievals derive the total mass of SO₂ within a volcanic cloud, whereas COSPEC values are measured as an SO₂ emission rate in tons per day). For this reason, a technique has been applied to the SO₂ maps to reproduce transects used by COSPEC so that a direct comparison can be tested.

Transects were made through the plume in the SO₂ map derived from the January 23, 2001 image taken at 0450 UTC.

Three transects of the lower cloud were taken and multiplied by a wind speed of 4.2 ms⁻¹, which was determined, from trajectory analysis, to be the wind speed at 7 km. Fig. 5 shows the location of the cloud and where the three transects were taken. SO₂ emissions of 5, 8, and 25 kT per day were determined for transects 1, 2, and 3 respectively (3 being the closest to the vent). Although no COSPEC data for this particular day

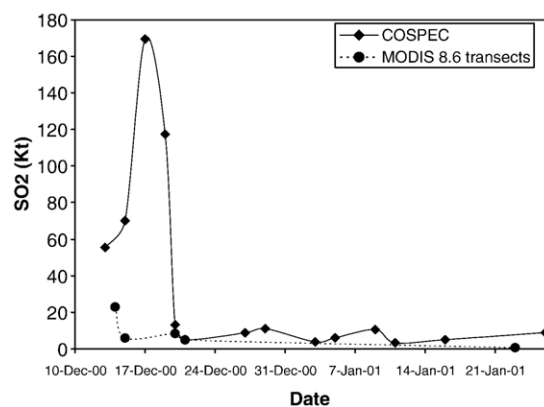


Fig. 6. COSPEC data taken from December 2000 to January 2001. The values of 5–8 kT per day, taken from the MODIS image, fall within the range of SO₂ fluxes for this period.

Table 6
Data for calculating SO₂ fluxes from MODIS images

MODIS image date and time	Transect distance from volcano (km)	Approximate speed (m/s)	Flux calculated (T/day)	Average flux (T/day)
12/14/00 17:50	3.) 38.5	1.8	7,500	23,000
	2.) 66	3.0	30,000	
	1.) 76.5	3.5	32,000	
12/15/00 16:55	3.) 22.5	0.5	3,000	6,000
	2.) 60	1.5	6,000	
	1.) 90	2.3	8,000	
12/20/00 05:05	3.) 32	0.4	3,400	8,500
	2.) 211	2.5	11,000	
	1.) 396	5.0	11,000	
12/20/00 17:15	3.) 94	0.7	5,000	5,000
	2.) 124	1.0	2,000	
	1.) 156	1.2	7,000	
01/23/01 17:00	3.) 22.5	0.3	300	750
	2.) 35	0.5	900	
	1.) 11.5	0.2	1,000	

Table 7
Data for calculating maximum volume of ejecta

Date and time	Column height (km)	Eruption duration (h)	Maximum volume of ejecta (m ³)
12/14/00 17:50	4	6.5	682,00
12/15/00 16:50	3	3	104,00
12/19/00 04:20	4	0.5	52,00
12/20/00 05:05	3	0.5	17,000
01/23/01 04:50	8	5.75	8,800,000

positively correlate with ash abundances. However, satellite sensors can only record the amount of ash and SO₂ in the cloud at the instant the image is acquired; they cannot quantify ash that has fallen out of the cloud or SO₂ that has dissipated to undetectable levels or reacted with H₂O to produce sulfates (Watson et al., 2004). This is a concern when attempting to compare the masses of SO₂ and ash as they have the potential to behave differently in the atmosphere.

The total volume of ejecta can be estimated using the column-height equation:

$$H = 1.67Q^{0.259}$$

where H is the column height and Q is the discharge rate of ash in cubic meters per second (Sparks et al., 1997). As the column heights for this eruption were carefully recorded, a discharge rate can be estimated. Knowing the eruption duration, we can then estimate a total mass of ash ejected within a single eruption. Table 7 lists the calculated total volume of ejecta for the explosions with MODIS data coverage. Column heights and eruption duration were taken from Popocatepetl observation notes from the Centro Nacional de Prevencion de Desastres (CENAPRED). The volume of ejecta appeared to decrease through the end of December and then to increase again as new activity ensued in January (Fig. 8).

A study on the magnetic anomalies for this period of activity (Martin-Del Pozzo et al., 2003) shows that magnetic precursors precede magma intrusion. According to their study, magnetic anomalies observed at end of December 2000 and January 2001 suggest that most of the magma was already emplaced by the December 14–15, 2000 eruptions, but was not erupted until the January 23, 2001 eruption. This may also explain why COSPEC values are much higher at the end of December than they are at the end of January 2001 (Fig. 6). If the magma was already in place, most of it could have degassed before the January 23, 2001 eruption (Martin Del Pozzo et al., 2003). This suggestion is reinforced by Fig. 8, which shows a much larger calculated volume of ejecta for the January 23, 2001 eruption than for those in December 2000.

5. Further work

This research should be extended to further test the limitations of the three retrieval processes used in this study. Algorithms for calculating SO₂ burdens within a given cloud using the absorption features of SO₂ at 8.6 μm and 7.3 μm are

were measured, these values do fall within the range of COSPEC data obtained during this period of activity (Fig. 6).

More transects from different days were taken to test if they would be comparable to COSPEC measurements. The wind speeds for these transects were also determined using trajectory analysis. Table 6 shows transects calculated from the MODIS images using upper wind data and the clouds distance from the volcano. The general trend of high SO₂ fluxes in mid-December 2000 and lower fluxes through the end of December 2000, as shown in Fig. 6, is also observed at the transects obtained from the MODIS data. These results illustrate that, although direct comparison of COSPEC and MODIS SO₂ data is not practical, transects taken from the MODIS data can be used with wind and observational data to obtain emissions of SO₂ similar to those measured by the COSPEC.

4.4. Comparison of ash retrievals to SO₂ retrievals

Comparing the MODIS ash retrievals to the MODIS 8.6 μm retrievals is important because, it might indicate a change in eruptive activity, or signify a developmental pathway for the eruption. As illustrated in Fig. 7, SO₂ abundances generally

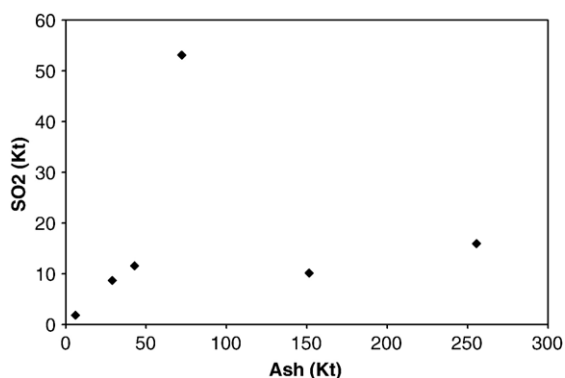


Fig. 7. Comparison of SO₂ and ash masses detected by MODIS images illustrating a general trend of increasing SO₂ values with increasing ash values.

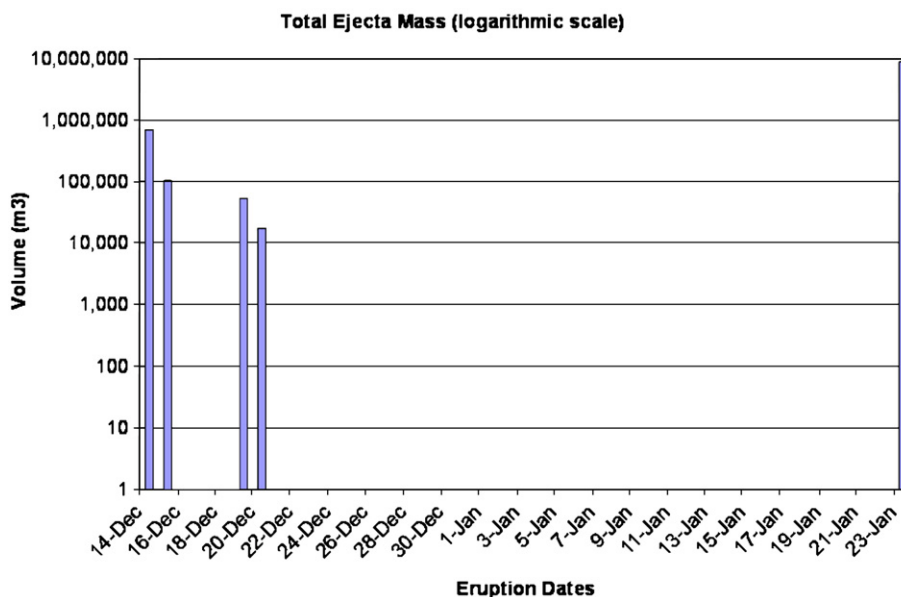


Fig. 8. Volume of ejecta for Popocatepetl Volcano during the December 2000 – January 2001 eruptive period.

currently being used for several different satellite sensors and for different volcanoes where environments are variable. These algorithms are being further tested to recognize their strengths and weaknesses under varying conditions and are undergoing constant modification. For example, studies have been undertaken on retrievals of emissions from Pacaya, Guatemala (Henney et al., submitted for publication) and Miyakejima, Japan (McCarthy et al., in press). As the limitations of the algorithms become more implicit, modifications can be made to allow them to be more useful to all the differing environmental and atmospheric settings.

Likewise, further testing of the algorithm for calculating the amount of ash in a volcanic cloud is also necessary to refine this algorithm, specifically a sensitivity study. This algorithm also has limitations that vary with atmospheric and environmental conditions and testing it under different circumstances could help us to enhance the effectiveness of this algorithm and make it more applicable to various volcanoes. This is important because the ash-detection algorithm is used operationally to track volcanic ash clouds to mitigate possible hazard to aircraft.

As illustrated in this research, Popocatepetl is an interesting volcano for testing these limitations because of the variety in both its ash and SO₂ emissions and the varying environmental and atmospheric conditions into which its volcanic clouds can be erupted. Enhancement of the algorithms to better deal with differing conditions can help us gain more accurate and reliable information about volcanic eruptions. The technique of quantifying emissions from MODIS SO₂ data using transects and wind data makes it possible to attempt to ground truth the SO₂ retrieval algorithms, as done with ASTER at Miyakejima (Urai et al., 2004), although it is challenging and many assumptions are required. Gathering contemporaneous ground-based and MODIS/ASTER data could potentially provide calibration and validation of the satellite-sensor data, which could generate more reliable studies of the origin and fate of volcanic clouds on

a larger scale. In addition, comparison of SO₂ with ash-emission data could be further developed to understand the complex physico-chemical relationships between the species of different phases.

6. Conclusions

Volcanic clouds erupted by Popocatepetl are large enough and high enough in altitude to be observed by the MODIS satellite sensor. Although meteorological conditions are not always ideal for the detection of volcanic clouds, those clouds that can be detected are easily visible in the images and can be analyzed using the 11 μm–12 μm retrieval (for ash) and the 8.6 μm retrieval process (for SO₂). Volcanic ash retrievals performed on MODIS and AVHRR images show general agreement between rates of SO₂ and ash emission but strongly suggest an early emission of SO₂ following shallow magma emplacement. AVHRR ash retrievals gave smaller ash masses than MODIS ash retrievals.

Although SO₂ is detectable within Popocatepetl's volcanic clouds, the 8.6 μm retrieval technique proved to be more suitable than the 7.3 μm retrieval for this study. This is because of the 7.3 μm retrieval's sensitivity to the altitude of the cloud as well as its limitations with respect to water vapor presence in the atmosphere. More testing of this algorithm is necessary to outline the limitations of the retrieval and to make it more functional in the context of a tropical atmosphere. Increases and decreases in the output of emissions by the volcano, as recorded by the MODIS sensor and the COSPEC, broadly agree.

Observational data and atmospheric wind profiles can be used with transects of MODIS SO₂ data to produce emission rates of SO₂ that can be compared to those measured by the COSPEC, and are of a similar magnitude. This shows that ground-based data could be supported by MODIS IR data, as previously suggested (Realmuto, 2000). Total mass of ejecta

was determined from column height and duration of eruption, and peaked (for the times of MODIS coverage) at $8.8 \times 10^6 \text{ m}^3$ during 23rd January (total production) at an average of $\sim 425 \text{ m}^3 \text{ s}^{-1}$. Satellite data can only provide information for the snapshot that the sensor is overhead, but facilitate quantification of inter-eruptive episodes. In contrast, ground-based data can yield SO_2 emission rates at any given time. It is challenging to relate the two types of data as they are necessarily dissimilar. It is, however, a valid exercise because: (a) the data provide quite different insights into volcanic activity; and (b) if satellite data can be manipulated to mimic ground-based transect data, then validation can be attempted. This is only possible at volcanoes where the scale of the eruption is quantifiable at both scales, which in reality is a fairly narrow window. The December 2000–January 2001 eruption of Popocatepetl represents the likely upper end of emission rate where this is possible. Better integration of the two types of measurement is required to make satellite-based monitoring of volcanic emissions robust, but it can be stated with some certainty that monitoring volcanic emissions from space is achievable and useful for many reasons.

Acknowledgements

We thank the Centro Nacional de Prevención de Desastres for support in facilitating access to data archives. Dr. Hugo Delgado-Granados acknowledges financial support from DGAPA-UNAM to spend part of a sabbatical leave at Michigan Technological University in order to initiate this collaborative work. Dr. Matthew Watson was funded in part for this research by NASA under NRA-03-OES-02.

References

- Alvarez, R., Ortiz, M.I., Gomez, G., Vidal, R., 2000. Geographic evaluation for hazardous volcanic emissions on population: the plumes of Popocatepetl in March 1996. Proc. Fourteenth International Conf. on Applied Geologic Remote Sensing, ERIM, pp. 255–262.
- Andres, R.J., Kasgnoc, A.D., 1998. A time-averaged inventory of subaerial volcanic sulfur emissions. *Journal of Geophysical Research* (ISSN: 0148-0227) 103. doi:10.1029/98JD02091 (D19).
- Delgado-Granados, H., Cardenas Gonzales, L., Piedad Sanchez, N., 2001. Sulfur dioxide emissions from Popocatepetl volcano (Mexico): case study of a high-emission rate, passively degassing erupting volcano. *Journal of Volcanology and Geothermal Research* 108, 107–120.
- Goff, F., Janik, C.J., Delgado, H., Werner, C., Counce, D., Stimac, J.A., Siebe, C., Love, S.P., Williams, S.N., Fischer, T., Johnson, L., 1998. Geochemical surveillance of magmatic volatiles at Popocatepetl volcano, Mexico. *Geological Society of America Bulletin* 110, 695–710.
- Henney, L.A., Watson, I.M. and Realmuto, V.J.R. The use of ASTER to detect volcanic sulfur dioxide emissions from Fuego and Pacaya volcanoes, Guatemala, submitted for publication to *Remote Sensing of Environment*.
- Love, S.P., Goff, F., Counce, D., Siebe, C., Delgado, H., 1998. Passive infrared spectroscopy of the eruption plume at Popocatepetl volcano, Mexico. *Nature* 396, 563–567.
- Martin-Del Pozzo, A.L., Cifuentes, G., Cabral-Cano, E., Bonifaz, R., Correa, F., Mendiola, I.F., 2003. Timing magma ascent at Popocatepetl volcano, Mexico, 2000–2001. *Journal of Volcanology and Geothermal Research* 125, 107–120.
- McCarthy, E.B., Bluth, G.J.S., Watson, I.M. and Andrew Tupper, Detection and analysis of the volcanic clouds associated with the August 18 and 28, 2000 eruptions of Miyakejima volcano, Japan, in press to *International Journal of Remote Sensing (Special Issue)*.
- Prata, A.J., 1989a. Observations of volcanic ash clouds in the 10–12 μm window using AVHRR/2 data. *International Journal of Remote Sensing* 10, 751–761.
- Prata, A.J., 1989b. Infrared radiative transfer calculations for volcanic ash clouds. *Geophysical Research Letters* 16, 1293–1296.
- Prata, A.J., Rose, W.I., Self, S., O'Brien, D., 2003. Global, long-term sulphur dioxide measurements from TOVS data: a new tool for studying explosive volcanism and climate. In: Robock, A., Oppenheimer, C. (Eds.), *AGU Special Publication on Volcanism and the Atmosphere*.
- Realmuto, V.J., 2000. The potential use of Earth observing system data to monitor the passive emission of sulfur dioxide from volcanoes. *Remote Sensing of Active Volcanism, Geophysical Monograph* 116, 110–115.
- Realmuto, V.J., Worden, H.M., 2000. Impact of atmospheric water vapor on the thermal infrared remote sensing of volcanic sulfur dioxide measurements: a case study from the Pu'u O'o vent of Kilauea Volcano, Hawaii. *Journal of Geophysical Research* 105, 21,497–21,508.
- Realmuto, V.J., Abrams, M.J., Boungiorno, M.F., Pieri, D.C., 1994. The use of multispectral thermal infrared image data to estimate the sulfur dioxide flux from volcanoes: a case study from Mount Etna, Sicily, July 29, 1986. *Journal of Geophysical Research* 99 (No. B1), 481–488.
- Realmuto, V.J., Sutton, A.J., Elias, T., 1997. Multispectral thermal infrared mapping of sulfur dioxide plumes: a case study from the East Rift Zone of Kilauea Volcano, Hawaii. *Journal of Geophysical Research* 102 (No. B7), 15,057–15,072.
- Sparks, R.S.J., Bursik, M.I., Carey, S.N., Gilbert, J.S., Glaze, L.S., Sigurdsson, H., Woods, A.W., 1997. *Volcanic Plumes*. John Wiley and Sons Ltd., West Sussex, England.
- Urai, M., 2004. Sulfur dioxide flux estimation from volcanoes using Advanced Spaceborne Thermal Emission and Reflection Radiometer — a case study of the Miyakejima volcano, Japan. *Journal of Volcanology and Geothermal Research* 134, 1–13.
- Watson, I.M., Realmuto, V.J., Rose, W.I., Prata, A.J., Bluth, G.J.S., Gu, Y., Bader, C.E., Yu, T., 2004. Thermal infrared remote sensing of volcanic emissions using the Moderate Resolution Imaging Spectroradiometer (MODIS). *Journal of Volcanology and Geothermal Research* 135, 75–89.
- Wen, S., Rose, W.I., 1994. Retrieval of sizes and total mass of particles in volcanic clouds using AVHRR bands 4 and 5. *Journal of Geophysical Research — Atmospheres* 99 (No. D3), 5421–5431.
- Yu, T., Rose, W.I., Prata, A.J., 2002. Atmospheric correction for satellite-based volcanic ash mapping and retrievals using “split-window” IR data from GOES and AVHRR. *Journal of Geophysical Research* 106 (No. D16), 10,1–10,19.